PERGAMON

Chemical Engineering Science 56 (2001) 2245–2253

Chemical Engineering Science

www.elsevier.nl/locate/ces

The effect of solvent on crystal growth and morphology

Meir Lahav, Leslie Leiserowitz*

Department of Materials and Interfaces, The Weizmann Institute of Science, Rehovot 76100, Israel

1. Introduction

Solvent has a strong influence on the habit of crystalline materials; however the role played by solvent–surface interactions in enhancing or inhibiting crystal growth is still not completely resolved. To date there have been two different approaches to clarify this point. In one theory, (Bennema & Gilmer, 1973; Bennema, 1992; Bourne & Davey, 1976; Elwenspoek, Bennema, & van Eerden, 1987) favorable interactions between solute and solvent on specific faces leads to reduced interfacial tension, causing a transition from a smooth to a rough interface and a concomitant faster surface growth. Alternatively, it has been proposed that preferential adsorption at specific faces will inhibit their growth as removal of bound solvent poses an additional energy barrier for continued growth. Studies on the role played by "tailor-made" additives on crystal morphology and inhibition of growth (Weissbuch, Addadi, Lahav, & Leiserowitz, 1991) are in keeping with the latter approach. The additive has the same structure as the host molecule but for an altered moiety. This moiety is designed so that the additive can be adsorbed only on a symmetry subset of crystallographic surface sites on specific faces. In such a way the adsorbed additive which essentially replaces a host molecule, is oriented such that the altered moiety emerges from the crystal surface. Such an adsorbed additive, therefore, would hinder regular deposition of oncoming molecular layers and so inhibit crystal growth at that face. Solvent–surface interactions cannot be as clearly analyzed as the interactions between the tailor-made additives and the crystal, since the solvent–surface geometry cannot be as well determined. In order to circumvent or overcome this problem we describe several approaches that have been adopted in order to establish the effect of solvent on crystal growth and morphology.

2. Characterization of solvent–surface interactions

One of the main difficulties is to disentangle the relative contributions of the internal crystal structure and solvent–surface interactions in determining the crystal morphology. The former may be evaluated by growing the crystal by sublimation, if possible, or by theoretical modeling. Such information has been used to understand the effect of solvent on crystal morphology. For example, the theoretical form of α-glycine (Berkovitch-Yellin, 1985; Boek, Feil, Briels, & Bennema, 1991) shown in Fig. 1a, is in good agreement with the morphology of α-glycine crystals obtained by sublimation (Fig. 1b). This morphology exhibits well-developed $\{0\,1\,0\}$ faces, in keeping with the dominant hydrogen-bonding energy of the molecular bilayer in the ac plane (Fig. 2a). But glycine crystals grown from aqueous solution display a distinctly different morphology that is bipyramidal, with large $\{0\,1\,1\}$ and $\{1\,1\,0\}$ faces and less well-developed $\{0\,1\,0\}$ faces (Fig. 2b). In order to understand these differences, substrate–solvent interaction were taken into account. The large $\{0\,1\,1\}$ and $\{1\,1\,0\}$ faces expose CO_2^- and NH_3^+ groups well oriented to have a strong affinity for water. The $\{0\,1\,0\}$ face exposes alternating layers of C–H groups or CO_2^- and NH_3^+ groups (Fig. 2a), and so, on average, is less hydrophilic than the $\{0\,1\,1\}$ and $\{1\,1\,0\}$ faces. These observations were expressed by Berkovitch-Yellin (1985) in a semi-quantitative form by calculating the Coulomb potential at the various faces, that indicated preferential adsorption of water molecules onto the polar $\{0\,1\,1\}$ and $\{1\,1\,0\}$ faces. Moreover, if the solute glycine molecules dock into surface sites primarily as cyclic hydrogen-bonded dimers, the $\{0\,1\,0\}$ face will essentially expose C–H groups. This hypothesis is supported by several observations. Diffusion coefficient measurements yielded an average size of the glycine cluster of 1.8 molecules in a supersaturated solution (Chang & Myerson, 1986; Myerson & Lo, 1990; Ginde & Myerson, 1992), but it was not established whether the clusters are in cyclic hydrogen-bonded form. Atomic force microscopy and phase measurement interferometric microscopy (Cai, Hillier, Franklin, Nunn, & Ward, 1994) yielded a step size of

* Corresponding author.

PII: S0009-2509(00)00459-0

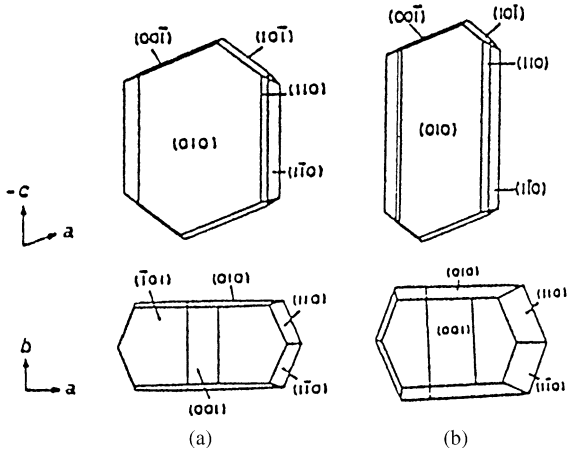

Fig. 1. (a) Theoretical crystal form of glycine. (b) Morphology of α-glycine crystals obtained by sublimation.

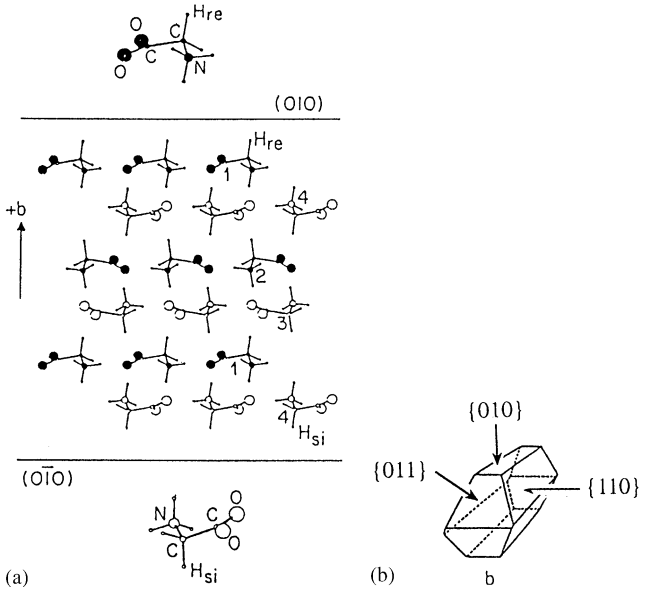

Fig. 2. (a) Packing arrangement of α-glycine viewed along the *a*-axis showing the four symmetry-related molecules; the C–H_{re} bonds, almost parallel to *b*, of the molecules point towards the (0 1 0) face and the corresponding C–H_{si} bonds towards the (0 −1 0) face. (b) Crystal morphology of α-glycine.

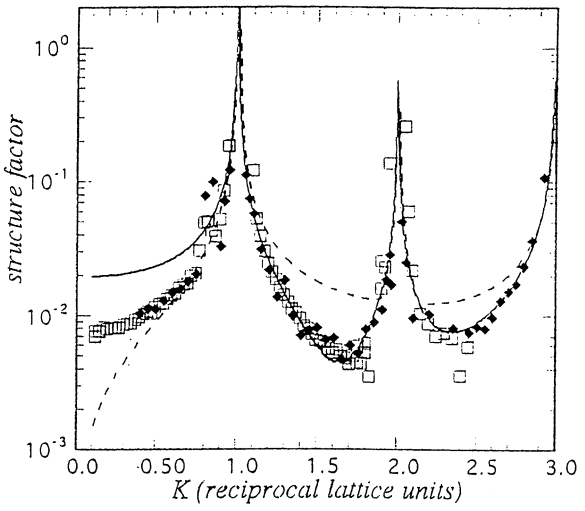

Fig. 3. Grazing incidence X-ray diffraction pattern of an α-glycine {0 1 0} surface during its growth from a saturated 0.75:0.25 ethanol–water solution. (Open squares) data points measured on the pure dry {0 1 0} cleaved surface. (Filled rhombus) data points measured in-situ during the growth of α-glycine. (Solid line) calculated model for the crystal terminated at the (0 1 0) face by the *a* layer exposing C–H groups. (Dashed line) calculated model for the crystal terminated by *a* layer exposing oxygen and NH groups.

≈1 nm at the growing (0 1 0) face of glycine, which corresponds to a thickness of the hydrogen-bonded glycine bilayer. Definitive evidence that a growing {0 1 0} face of α-glycine in an aqueous glycine solution exposes primarily C–H groups came from an in situ monitoring of the structure of the (0 1 0) face by grazing incidence X-ray diffraction measurements (Fig. 3) using synchrotron radiation (Gidalevitz, Feidenhans'l, & Leiserowitz, 1997). Further support for the arguments that the {1 1 0} and {0 1 1} crystal faces of glycine are enhanced by their interactions with water comes from the observed crystal morphology of the α-amino acids with hydrophobic chains such as phenyl alanine (Weissbuch, Frolow, Addadi, Lahav, & Leiserowitz, 1990), valine, isoleucine (Torri & Iitaka, 1970, 1971). Their crystal structures are composed of hydrogen-bonded bilayers as in α-glycine and their morphologies are plate-like when grown from aqueous solution. Clearly, the hydrophobic chains provide increased layer energy and a lower binding concentration of water at the sides of such bilayers than in α-glycine, providing a strong propensity for plate formation.

3. Crystalline solvates

Another approach involved the use of crystalline solvates where the solvent of crystallization plays the dual role of solvent and crystal solute. Such crystals were grown in the added presence of tailor-made solvent, which is slightly modified version of the solvate solvent. It was found when crystalline hydrates were grown from aqueous solution in the added presence of methanol (the "tailor-made" solvent), that the change in morphology was interpretable (Shimon, Vaida, Addadi, Lahav, & Leiserowitz, 1990, 1991) in a manner akin to the effect of a tailor-made inhibitor. This approach is illustrated with the crystal of α-rhamnose monohydrate, which contains a polar arrangement (Fig. 4a) in space group $P2_1$ and, when grown from pure aqueous solution, displays a bipyramidal morphology (Fig. 4b). The two O–H bonds of

the hydrate water molecules are oriented towards the $+b$-direction, but not towards the $-b$-direction of the crystal. Thus addition of methanol, as a co-solvent, changes the morphology of the crystal completely inhibiting growth along the $+b$-direction yielding a pyramidal crystal (Fig. 4c).

A second example is (*S*)-asparagine–H_2O. Crystals grown from pure water solution are delineated by 18 faces (Fig. 5b). The packing arrangement (Fig. 5a) shows that one of the two O–H bonds of each water molecule emerges from the $\{0\,1\,0\}$ faces, which are poorly expressed. Therefore, methanol molecules can be easily attached at these surface sites (Fig. 5a). The methyl groups of these adsorbed molecules protrude from the two $\{0\,1\,0\}$ faces, impede growth in the *b*-direction and thus induce formation of large $\{0\,1\,0\}$ crystal faces (Fig. 5b). On the $\{0\,1\,1\}$ faces, only two of the four symmetry-related molecules can be substituted by methanol and so inhibition of $\{0\,1\,1\}$ should be less dramatic. This reasoning proved to be in keeping with experiment (Shimon et al., 1991); growth in the presence of methanol as additive yielded $\{0\,1\,0\}$ plates similar in shape as when asparagine is grown in the presence of aspartic acid (Fig. 5b). That methanol can indeed be selectively adsorbed on both the $\{0\,1\,0\}$ and $\{0\,1\,1\}$ faces was further demonstrated by experiments involving partial dissolution of asparagine–H_2O crystals in methanol solution, revealing etch pits, although poorly developed, on only these faces (Shimon, Lahav, & Leiserowitz, 1986).

4. Polar crystals

In another approach, use was made of the principle that in a polar crystal the molecular attachment energy E_{att} at opposite and hemihedral faces $(h\,k\,l)$ and $(-h\,-k\,-l)$ are the same (neglecting the effects such as possible differences in molecular charge density in the bulk and to be-attached molecules at the opposite faces). Although a difference in these E_{att} has been invoked to explain the polar morphology of urea obtained by sublimation (Docherty, Roberts, Saunders, Black, & Davey, 1993), its effect on morphology must be far less than that of solvent on crystal growth and morphology. Thus, in the absence of a difference in the effect of binding of solvent at the hemihedral faces $(h\,k\,l)$ and $(-h\,-k\,-l)$, these two faces should grow at the same rate (Turner & Lonsdale, 1950). A pronounced difference in growth

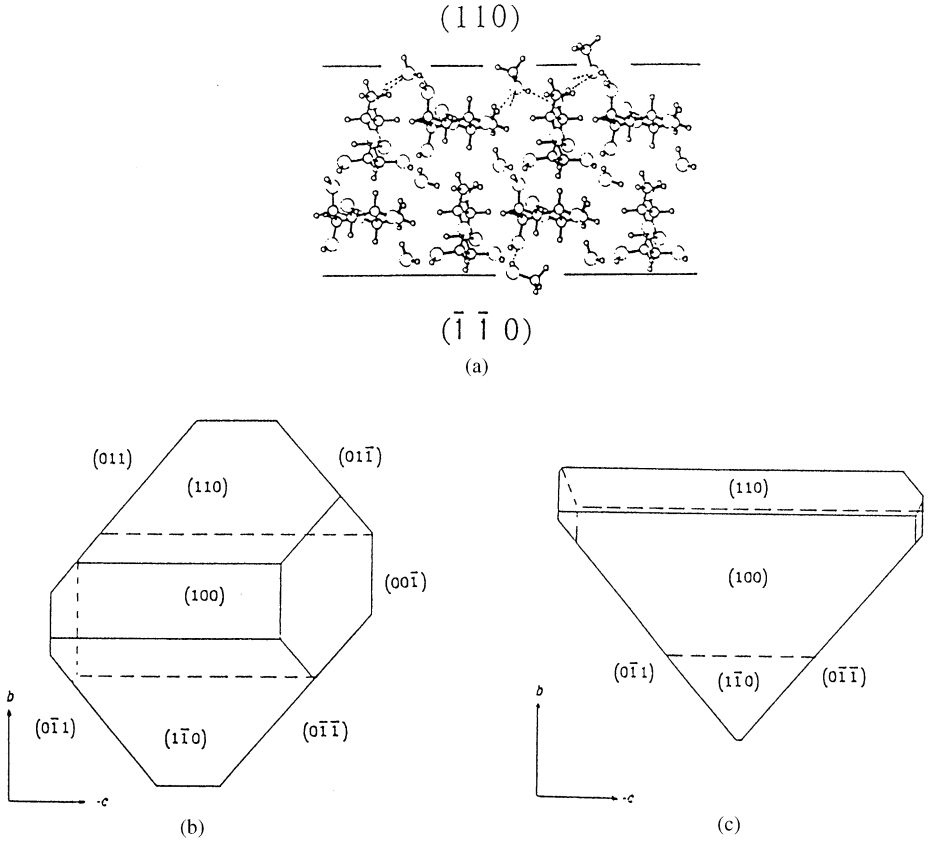

Fig. 4. (a) Packing arrangement of α-rhamnose monohydrate crystal viewed along the *a*-axis; the OH bonds of the hydrate water molecules point towards the $+b$, but not the $-b$ direction; replacement of water by methanol on the $\{1\,1\,0\}$ faces is depicted. (b)–(c) Crystal morphologies of α-rhamnose monohydrate grown from: (b) aqueous solution; (c) 9:1 methanol:water solution.

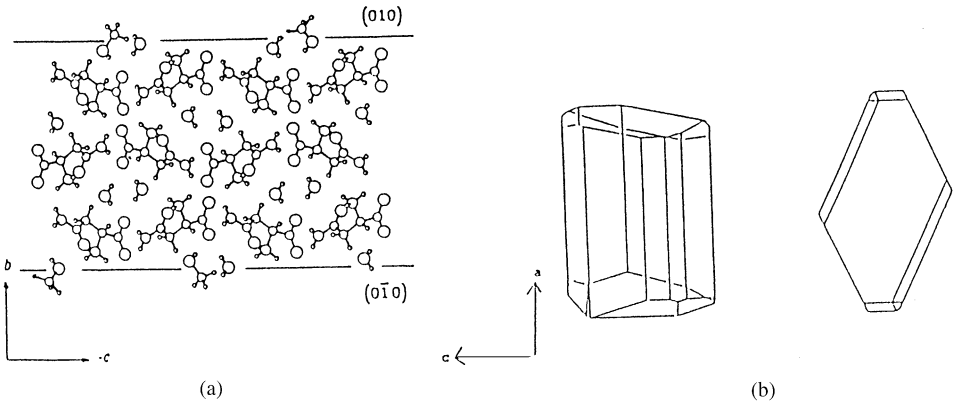

Fig. 5. (a) Packing arrangement of (*S*)-asparagine monohydrate viewed along the *a*-axis. Four adsorbed methanol molecules are inserted on the two $\{0\,1\,0\}$ faces, referring to crystals grown from water–methanol solution. (b) Morphologies of (*S*)-asparagine monohydrate. Left: Pure crystal grown from aqueous solution. Right: Crystal grown from a methanol–water solution.

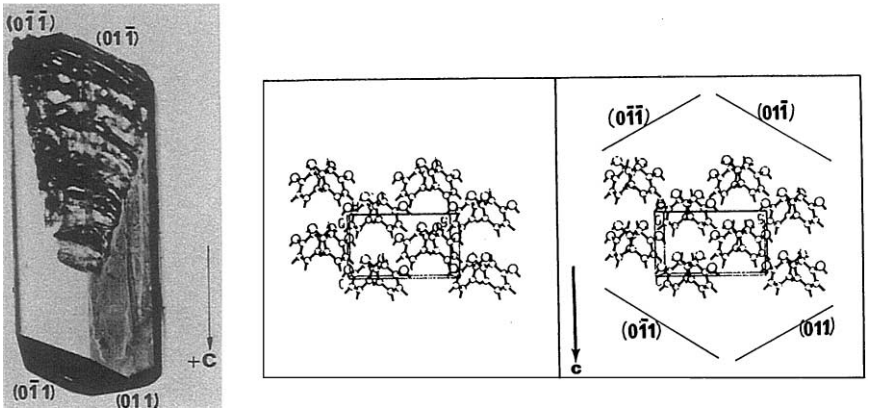

Fig. 6. Left: Typical crystal of α-resorcinol grown from water. The end faces $\{0\,1\,1\}$, i.e. $(0\,1\,1)$ and $(0\ -1\,1)$, and $\{0-1-1\}$ i.e. $(0-1-1)$ and $(0\,1\ -1)$, are marked. Right: Packing arrangement of α-resorcinol, Stereoscopic view along the *a*-axis. The planes parallel to the 'phenyl-rich' $\{0\,1\,1\}$ and hydroxy-rich $\{0-1-1\}$-faces are denoted.

rate must then be associated with differences in solvent–surface interactions.

About 50 years ago, Wells (1949) reported a benchmark study on the effect of solvent on growth of polar crystals. He found that in aqueous solution, the α-form of resorcinol (1,3-dihydroxybenzene), which crystallizes in space group $Pna2_1$, grows unidirectionally along the polar *c*-axis in aqueous solution (Fig. 6, left). Wells tried to correlate this experimental result with the observation that the crystal exposes "phenyl-rich" $(0\,1\,1)$ and $(0\ -1\,1)$, labeled $\{0\,1\,1\}$, faces at one end of the *c*-axis and "hydroxy-rich" $(0\,1-1)$ and $(0-1-1)$ faces, i.e. $\{0\ -1\ -1\}$, at the opposite end (Fig. 6, right). But Wells did not know which end of any specimen crystal was phenyl-rich and which end hydroxy-rich, since the absolute polarity of the crystal could not be ascertained at that time. Wells interpreted the unidirectional growth along *c* to take place at the phenyl-rich faces as a result of stronger adsorption of water to the hydroxy-rich faces.

The problem of determination of absolute polarity of α-resorcinol crystals bedeviled the investigation by Davey, Bourne, and Milisavljevic (1988), although they had made an assignment via oriented growth of resorcinol on silica surfaces. This assignment was made unambiguously by growth experiments of resorcinol in aqueous solution in the presence of tailor-made additives (Wireko et al., 1987). The unidirectional growth takes place at the hydroxy-rich $\{0-1-1\}$ faces. In order to help explain this fact, it was preferable to consider the $\{0\,1\,1\}$ face as acidic and corrugated and the $\{0-1-1\}$ face as basic and flat (Fig. 7). The "proton-donor" nature of the $\{0\,1\,1\}$ face is evident since it exposes per lattice repeat one O–H bond and four C–H bonds that may participate in attractive C–H–O (water) interactions. The corrugated nature of the $\{0\,1\,1\}$ face suggested that water molecules may be adsorbed within the pockets. The "proton-acceptor" properties of the $\{0-1-1\}$ face arise from the fact that three out of four resorcinol oxygen atoms form

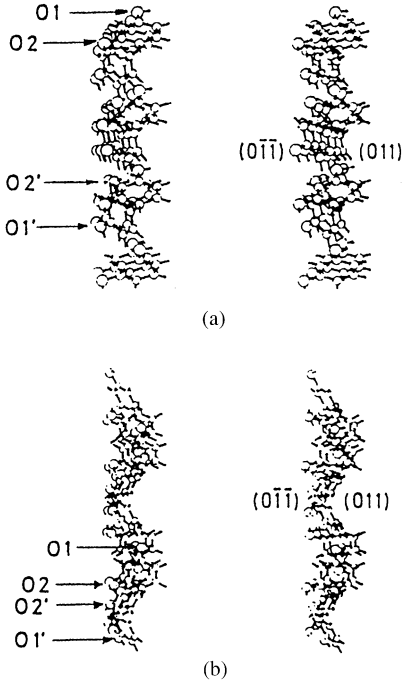

Fig. 7. Resorcinol. Two different views of an 0 1 1 molecular layer showing the surface structures at the (0 1 1) and (0 −1 −1) faces: (a) along the *a*-axis; (b) along the direction $-b+c$.

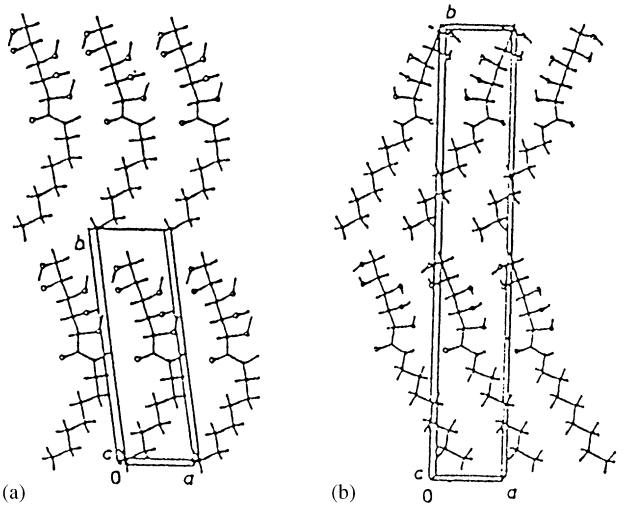

Fig. 8. Head-to-tail packing arrangement of: (a) *N*-(*n*-heptyl)-(D)-gluconamide in space group P1; (b) *N*-(*n*-octyl)-(D)-gluconamide in space group $P2_1$.

intralayer O–H–O bonds and are accessible to water at this face. These observations, however, were insufficient for a quantitative prediction of preferred growth along the polar axis (Wireko et al., 1987; Davey et al., 1988). Nevertheless, this problem provided incentive for a general study how solvent affects crystal growth described herein, and more recently, for a molecular simulation analysis of the effect of water on the faces of α-resorcinol by Hussain and Anwar (1999) and which indeed accounted for its growth behavior. Their analysis indicates that the adsorption of water is stronger at the slower growing {0 1 1} sites.

The principle that a pronounced difference in growth rate at opposite hemihedral faces of a polar crystal must be associated with differences in their solvent–surface interactions was exploited in the family of plate-like crystals composed of enantiomeric alkylgluconamides $C_nH_{2n+1}NHCO(CHOH)_4CHOH$, $n = 7$–10. In the two crystal structures for $n = 7,8$ (Fig. 8) reported by Zabel et al. (1986), the molecules pack in layers stacked head-to-tail in a polar arrangement (chain-like amphiphilic molecules normally pack head-to-head and tail-to-tail in the crystalline state). Thus the polar plate-like crystals are hydrophobic at one plate face and hydrophilic at the opposite face. Our notion was first to ascertain the relative binding strengths of polar solvents to the opposite hemihedral faces from their macroscopic wetting properties, as determined by contact angle measurements (Wang, Lahav, & Leiserowitz, 1991). Next the object was to correlate this information with the relative rates of growth of the two crystal faces in the same solvents (Wang, Leiserowitz, & Lahav, 1992). These contact angle measurements established that polar solvents wet the hydrophilic face more strongly than the opposite hydrophobic face. Furthermore, in CH_3OH solution the polar plate-like crystals of the octyl derivative ($n = 8$) were found to grow almost four times faster at the hydrophobic side than at the hydrophilic side (Fig. 9), a result completely in keeping with the wetting properties of the crystal faces. It is noteworthy that at the hydrophilic face, solvent methanol can form O–H–O hydrogen bonds with the terminal hydroxyl groups of two neighboring chains, since the separation distance between them is about 5 Å. Calculations by Khoshkoo and Anwar (1996), of the average solvent binding energy to the different crystal faces, is in full agreement with observation.

The theory that strong solvent–surface interactions inhibit crystal growth is also borne out by a comparison of the effect of tailor-made additives and acetic acid solvent on the morphology of the polar crystals of *N*-(cinnamoyl)-alanine (Berkovitch-Yellin, Addadi, Idelson, Leiserowitz, & Lahav, 1982; Shimon et al., 1991).

5. A "relay" mechanism of crystal growth

An entirely different approach involved strong selective adsorption of solvents at a subset of molecular surface sites, of, say, type B and repulsion of solvent at the remaining set of surface sites of, say, type A on the crystal face. This is depicted in Scheme 1, where we emphasize the difference between the two types of sites by assuming a corrugated surface such that the A-type site is a cavity and the B-type site is on the outside upper surface of the

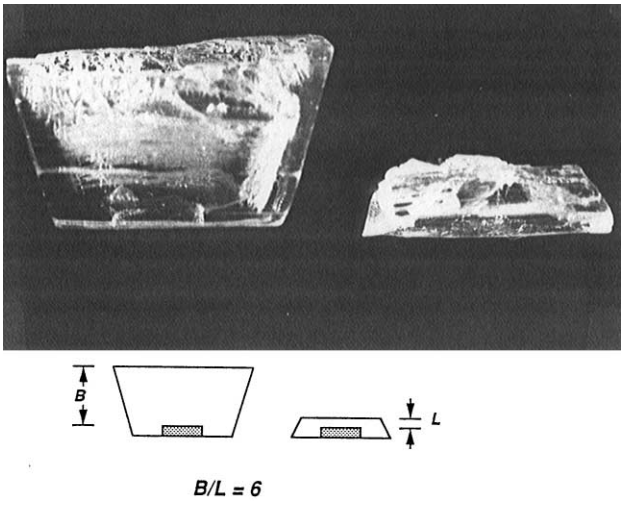

Fig. 9. Morphology of *N*-*n*-octylgluconamide crystal grown from methanol. The seeds can be observed as an opaque shadow at the bottom of the crystals. Thickness of added material on the hydrophobic surface is denoted as B and that added on the hydrophilic surface is denoted as L. The B/L ratio has an average value of about 5.

cavity. Scheme 1a shows the B-type sites blocked by solvent S and the A-type sites unsolvated. Thus solute molecules can easily fit into A-type sites. But once docked into position (Scheme 1b), the roles of the A- and B-type sites are essentially reversed and the solvent molecules which originally were bound to B-type sites would be repelled since they now occupy A-type sites. This cyclic process can lead to fast growth by a kind of "relay" mechanism. In such a situation described here, where desolvation is rate limiting, we have implicitly made use of the idea that the free energy of incorporation of a solute molecule helps to displace bound solvent. This relay mechanism may be demonstrated by a crystal with a polar axis and the experiment involves a comparison of the relative rates of growth at the opposite poles for the different solvents, as exemplified by the growth and dissolution of the crystals of (R,S)-alanine and γ-form of glycine in different solvents (Shimon et al., 1990,1991). These two crystals have similar packing features and so the discussion is limited to (R,S)-alanine. The zwitterionic molecules are aligned so as to expose CO_2^- groups at one end of the polar c-axis and NH_3^+ groups at the opposite end (Fig. 10). The crystal has a polar morphology, with the CO_2^- groups emerging at the flat $-c$ end (Fig. 10), as determined by partial dissolution of crystalline (R,S)-alanine in the presence of tailor-made additives, resulting in etch-pit formation (Shimon et al., 1986). The $(0\,0\,-1)$ face at the carboxylate end contains cavities. This face grows and dissolves faster in aqueous solution than the "smoother" amino face (Fig. 11a). We propose that the faster growth at the $(0\,0-1)$ side of the crystal in aqueous solution is due to the relay mechanism of growth, according to the following arguments.

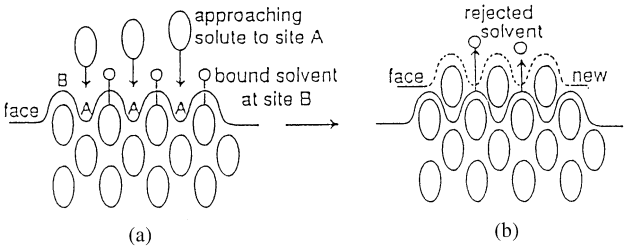

Scheme 1.

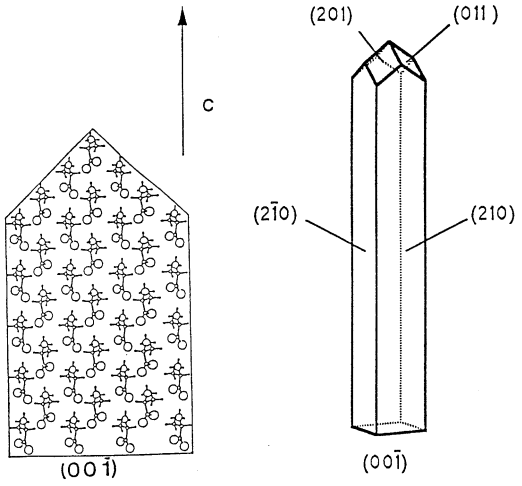

Fig. 10. Packing arrangement of (R,S)-alanine delineated by crystal faces, as viewed down the b-axis. The capped faces at the $+c$ end of the polar axis expose NH_3^+ and $-CH_3$ groups at their surfaces, the opposite $(0\,0\,l)$ face exposes carboxylate CO_2^- groups.

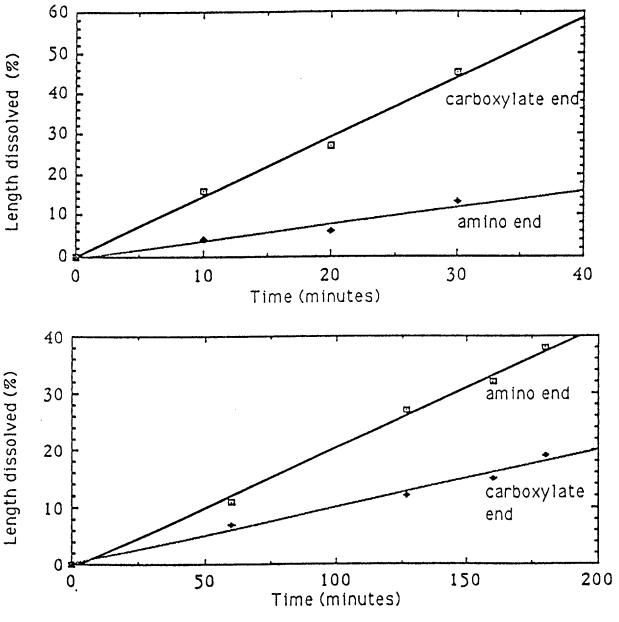

Fig. 11. Graph of the relative growth at the opposite poles of the polar axis of (R,S)-alanine crystals: (a) in water; (b) in 4:1 methanol:water mixture.

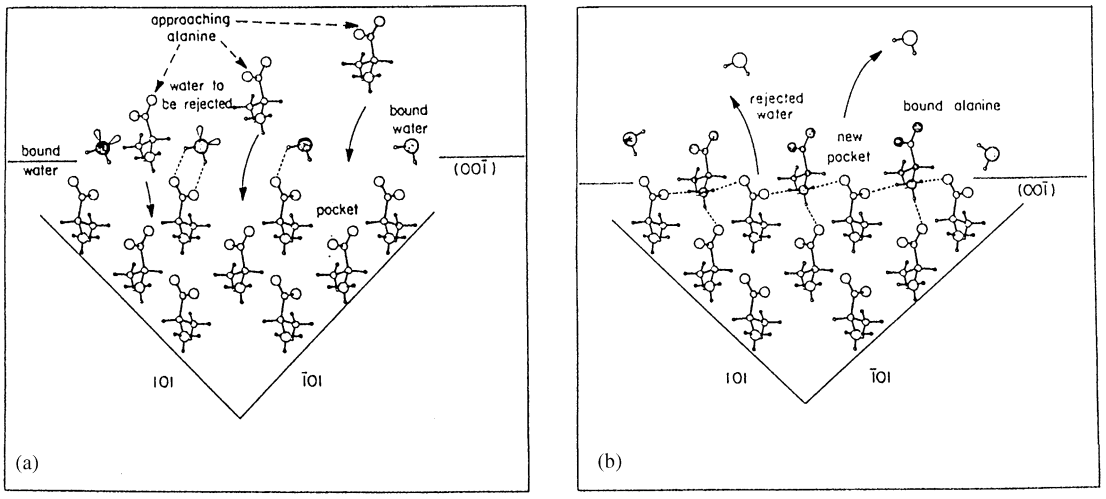

Fig. 12. Schematic representation of the (0 0 − 1) face of *R*, *S*-alanine during crystal growth. (a) In this view approaching solute alanine molecules are depicted about to be bound within the pockets of the (0 0 − 1) face. Also shown are water molecules bound to the outermost CO_2^- groups of this face. (b) In this view, the newly adsorbed alanine molecules are each bound via three NH–O hydrogen bonds. The previously bound water molecules are shown being rejected by O(water)–O(carboxylate) lone pair–lone pair repulsions. Note the formation of new unsolved pockets.

The water molecules may be strongly bound by hydrogen bonds to the outermost layer (0 0 −1) of CO_2^- groups. In contrast, the pockets act as proton acceptors for the NH_3^+ groups of the solute molecules. Replacement of the solute NH_3^+ moiety by solvent water within the pockets yields repulsive or, at best, weakly attractive interactions. The pockets will, therefore, be weakly hydrated and so relatively easily accessible to approaching solute molecules (Fig. 12). There is, however, an alternative mechanism which may account for the faster growth at the − *c* end: a higher crystal attachment energy at the (0 0 −1) end of the crystal than at the opposite end. We could demonstrate that the relay mechanism is the more operative on the following prediction: methanol, as cosolvent, should be able to bind into the pocket by virtue of attractive, albeit weak, C–H(methanol)–O(carboxylate) interactions and an O–H(methanol)–O(carboxylate) hydrogen bond at the surface of the pocket, and thus reduce the growth rate at the (0 0 −1) face. Indeed, crystals of (*R*, *S*)-alanine in 80% methanol:water mixture were found to grow faster at the + *c* amino end of the crystal than at the − *c* carboxylate end (Fig. 11b), indicating that methanol blocks solute access to the pockets more effectively than water at the (0 0 −1) face.

This work implies that for those crystals that expose sets of different surface sites at each face, the average binding energy of solvent to a face may not be a sufficient criterion for establishing the relative morphological importance of the different faces. It may be necessary to assess the ease of replacement of solvent by solute at each of the different surface sites, as well as the different modes of docking the solute molecules at the surface. For example, Boek et al. (1991) calculated the theoretical growth form of tetragonal urea and found that it is almost cube like and compares well with those of crystals from ethanol or benzene. But the theoretical form is very different in shape from the [0 0 1] needles obtained from aqueous solution. Boek and Briels (1992) performed molecular dynamics simulations of interfaces between water and crystalline urea. They argued that the observed

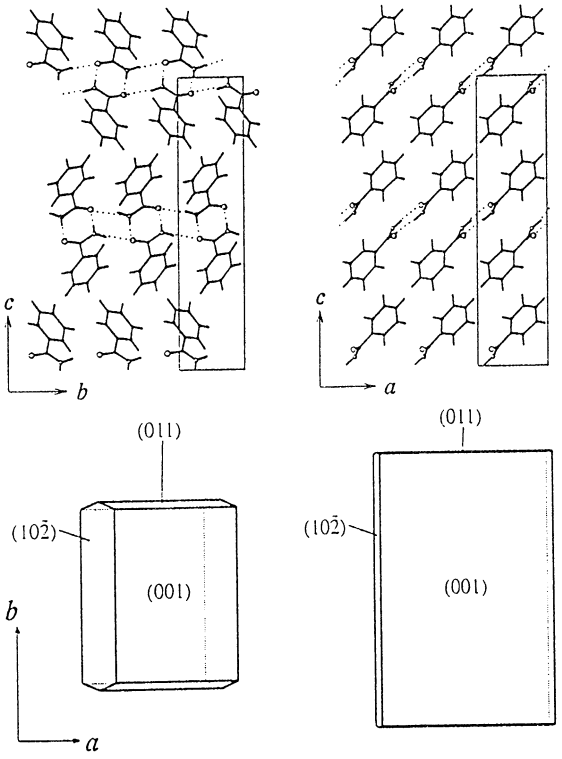

Fig. 13. Top: two views of the packing arrangement of benzamide (NH–O hydrogen bonds denoted by dashed lines). Bottom: Benzamide morphology, Left: pure form. Right: grown from an equimolar benzamide–amide cosolvent solution (acetamide, trifluoroacetamide or chloroacetamide).

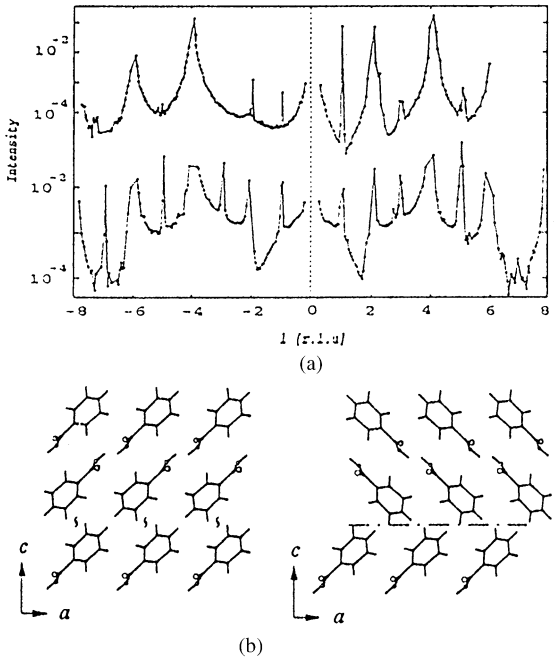

Fig. 14. (a) The (1 0 *l*) diffraction pattern measured from the (0 0 1) face of (top) pure benzamide and (botttom) grown in a 1:1 benzamide–trifluoroacetamide solution. (r.l.u = reciprocal lattice units). (b) Interlayer arrangement of benzamide viewed along the *b*-axis. Left: original structure in which the layers are related by 2_1 symmetry (denoted by symbol). Right: The layers are related by the proposed *n*-glide yielding twinning about the *n*-glide plane (dash-dot line).

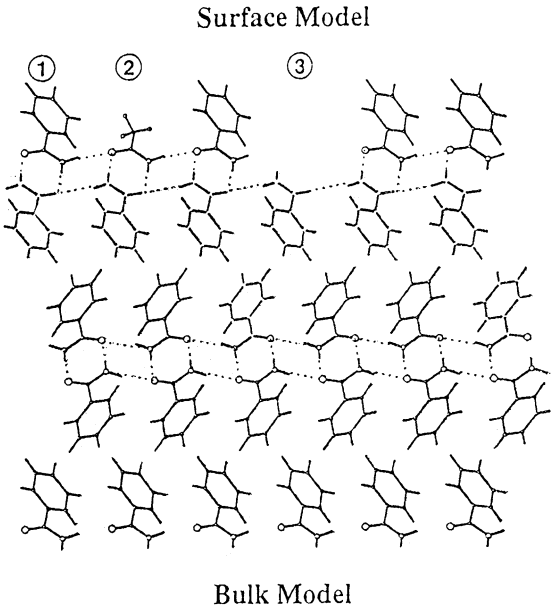

Fig. 15. Bulk and surface models used for X-ray structure factor calculations of the pure and affected benzamide crystals. The top surface layer is occupied by: (1) benzamide molecule, (2) amide cosolvent, or (3) empty space.

needle morphology cannot be explained using a simple layer model because of strong adsorption of water to the relevant faces. By examining the interface between a saturated aqueous urea solution and crystalline urea, Boek (1991) explained the [0 0 1] needle morphology in terms of wrongly and randomly absorbed urea molecules to the {1 1 0} side faces, so providing an increased interfacial entropy.

6. Solvent-induced twinning of crystals

Not only can solvent affect the nucleation, growth, and morphology of a crystal, but also its twinning behavior, according to the crystallization of saccharin (Williams-Seton, Davey, & Lieberman, 1999). and of benzamide from different solvents (Edgar, Schultz, Rasmussen, Feidenhans'l, & Leiserowitz, 1999). Saccharin tends to form single twins at the nucleation stage whereas benzamide forms lamellar twins during growth.

Single crystals of benzamide, which form hydrogen-bonded (0 0 1) bilayers (Fig. 13, top), are obtained from ethanol or propanol solutions. The added presence of amide co-solvents such as $X–CONH_2$, $X = CH_3$ or CF_3, yields very thin (0 0 1) plates which are twinned. Analysis of the grazing incidence X-ray diffraction (GIXD) measurements from the (0 0 1) surface of the pure crystals indicated that the surface almost exclusively exposed the phenyl substituents as shown in Fig. 13 (top). This result is in keeping with, but not a proof of, the docking from solution of cyclic hydrogen-bonded dimers onto the (0 0 1) surface. GIXD measurements of the (0 0 1) faces of the pure and affected crystals as shown in Fig. 14a revealed lamellar twinning of the latter. The (1 0 *l*) diffraction pattern of the pure crystal (Fig. 14a, top) shows no symmetry about the Miller index *l* in keeping with the space group symmetry of a single crystal. On the other hand, the (1 0 *l*) diffraction pattern of the affected crystal (Fig. 14a, bottom) is symmetric about the Miller index *l*. This result can be simply explained in terms of the formation of several twinned lamellae each of about a micron thickness since the penetration depth of the X-ray beam into the specimen crystal was about 30 μm. Structural modeling of the (0 0 *l*) diffraction pattern from the surface of a twinned crystal showed that the top (0 0 1) surface layer contained about 15% stereospecifically-adsorbed amide cosolvent molecules, in contrast to the 1% amide cosolvent in the bulk, as revealed by chemical analysis. The cosolvent occupies only those surface sites whose X moieties emerge from the crystal and not the centrosymmetrically-related counterpart as shown in Fig. 15. Thus the affected (0 0 1) surface can be regarded as composed of phenyl rings and random sites occupied by amide cosolvent exposing cavities. A model was proposed that the lamellar twinning was induced by the presence of amide cosolvents on the (0 0 1) face in

a concentration sufficiently large to lower the interlayer specificity. Thus the oncoming benzamide layer may dock into position via a pseudo *n* glide (Fig. 14b, right) rather than via the regular two-fold screw axis as shown in Fig. 14b (left).

7. Outlook

The role played by solvent on crystal growth and dissolution and morphology is gradually being unraveled. We may expect that in the coming years experimental and computational efforts will be made in order to help clarify the role of solvent on crystal nucleation and polymorphism.

References

Bennema, P. (1992). *Journal of Crystal Growth*, *122*, 110–119.

Bennema, P., & Gilmer, G. (1973). In P. Hartman (Ed.) *Crystal growth: an introduction* (pp. 263–327). Amsterdam: North-Holland.

Berkovitch-Yellin, Z. (1985). *Journal of the American Chemical Society*, *107*, 8239–8253.

Berkovitch-Yellin, Z., Addadi, L., Idelson, M., Leiserowitz, L., & Lahav, M. (1982). *Nature*, *296*, 27–34.

Boek, E. S. (1991). *Crystal-solution interfaces*. Ph.D. thesis, University of Twente, The Netherlands.

Boek, E. S., & Briels, W. J. (1992). *Journal of Chemical Physics*, *96*, 7010–7018.

Boek, E. S., Feil, D., Briels, W. J., & Bennema, P. (1991). *Journal of Crystal Growth*, *114*, 389–410.

Bourne, J. R., & Davey, R. J. (1976). *Journal of Crystal Growth*, *36*, 278–286.

Cai, H., Hillier, A. C., Franklin, K. R., Nunn, C. C., & Ward, M. D. (1994). *Science*, *266*, 1551–1555.

Chang, Y. C., & Myerson, A. S. (1986). *American Institute of Chemical Engineers*, *32*, 1746–1749.

Davey, R. J., Milisavljevic, B., & Bourne, J. R. (1988). *Journal Physical Chemistry*, *92*, 2032–2036.

Docherty, R., Roberts, K., Saunders, V., Black, S., & Davey, R. J. (1993). *Faraday Discussions*, *95*, 11–26.

Elwenspoek, M., Bennema, P., & van Eerden, J. P. (1987). *Journal of Crystal Growth*, *83*, 297–305.

Edgar, R., Schultz, T., Rasmussen, F. B., Feidenhans'l, R., & Leiserowitz, L. (1999). *Journal of the American Chemical Society*, *121*, 632–637.

Gidalevitz, D., Feidenhans'l, R., & Leiserowitz, L. (1997). *Angewandte Chemie*, *36*, 959–962.

Ginde, R. E., & Myerson, A. S. (1992). *Journal of Crystal Growth*, *116*, 41–47.

Hussain, M., & Anwar, J. (1999). *Journal of the American Chemical Society*, *121*, 8583–8591.

Khoshkoo, S., & Anwar, J. (1996). *Journal of Chemical Society, Faraday Transactions*, *92*, 1023–1025.

Myerson, A. S., & Lo, P. Y. (1990). *Journal of Crystal Growth*, *99*, 1048–1052.

Shimon, L. J. W., Lahav, M., & Leiserowitz, L. (1986). *Nouveau J. Chem.* (*Special Issue*). *10*, *723–737*.

Shimon, L. J. W., Vaida, M., Addadi, L., Lahav, M., & Leiserowitz, L. (1990). *Journal of the American Chemical Society*, *112*, 6215–6220.

Shimon, L. J. W., Vaida, M., Addadi, L., Lahav, M., & Leiserowitz, L. (1991). IUCR crystallographic symposia, vol. 4, In J. B. Gabarczyk, & D. W. Jones (Eds.), *Organic crystal chemistry* (pp. 74–99). Oxford: Oxford University Press.

Torri, K., & Iitaka, Y. (1970). *Acta Crystallographica*, *B26*, 1317–1326.

Torri, K., & Iitaka, Y. (1971). *Acta Crystallographica*, *B27*, 2237–2246.

Turner, E., & Lonsdale, K. (1950). *Journal of Chemical Physics*, *18*, 156.

Williams-Seton, L., Davey, R. J., & Lieberman, H. F. (1999). *Journal of the American Chemical Society*, *121*, 4563–4567.

Wang, J. L., Lahav, M., & Leiserowitz, L. (1991). *Angewandte Chemie, Internation Edition*, *30*, 696–698.

Wang, J. L., Leiserowitz, L., & Lahav, M. (1992). *Journal of Physical Chemistry*, *96*, 15–16.

Weissbuch, I., Addadi, L., Lahav, M., & Leiserowitz, L. (1991). *Science*, *253*, 637–645.

Weissbuch, I., Frolow, F., Addadi, L., Lahav, M., & Leiserowitz, L. (1990). *Journal of the American Chemical Society*, *112*, 7718–7724.

Wells, A. F. (1949). *Discussion of the Faraday Society*, *5*, 197–201.

Wireko, F. C., Shimon, L. J. W., Frolow, F., Berkovitch-Yellin, Z., Lahav, M., & Leiserowitz, L. (1987). *Journal of Physical Chemistry*, *91*, 472–481.

Zabel, V., Muller-Fahrnow, M., Hilgenfeld, R., Saenger, W., Pfannemuller, B., Enkelmann, V. L., & Welke, W. (1986). *Chemistry of Physics of Lipids*, *39*, 313–327.